ResearchGate

See discussions, stats, and author profiles for this publication at: https://www.researchgate.net/publication/281445063

Optimization and control of one dimensional packed bed modelof underground coal gasification

Article *in* Journal of Process Control · November 2015

DOI: 10.1016/j.jprocont.2015.08.002

CITATIONS
18

READS
362

5 authors, including:

Ali Arshad
COMSATS University Islamabad
39 PUBLICATIONS **364** CITATIONS
SEE PROFILE

Aamer Iqbal Bhatti
University of Engineering & Technology Lahore
245 PUBLICATIONS **2,091** CITATIONS
SEE PROFILE

Erum Aamir
5 PUBLICATIONS **92** CITATIONS
SEE PROFILE

Raza Samar
Capital University of Science & Technology
71 PUBLICATIONS **1,419** CITATIONS
SEE PROFILE

All content following this page was uploaded by Ali Arshad on 28 May 2022.

The user has requested enhancement of the downloaded file.

Optimization and control of one dimensional packed bed model of underground coal gasification

Ali Arshad Uppal[a], Aamer Iqbal Bhatti[b], Erum Aamer[b], Raza Samar[b], Shahid Ahmed Khan[a]

[a] *COMSATS Institute of Information Technology, Islamabad, Pakistan*
[b] *Mohammad Ali Jinnah University, Islamabad, Pakistan*

Abstract

This paper discusses the optimization and control of the one dimensional (1-D) packed bed model of underground coal gasification (UCG) process for an actual UCG site. The optimization is performed to compensate for the uncertainty in coal and char ultimate analysis (caused by repeated measurements of different samples) and in steam to oxygen (O_2) ratio at the reaction front. The constrained nonlinear optimization problem is solved by using state of the art sequential quadratic programing (SQP) algorithm to minimize the error between experimental and simulated heating values. The results of the optimized model are validated with actual filed trials which show a good match for heating value of the product gases. The super twisting controller, a second order sliding mode control (SOSMC) algorithm is successfully implemented on the process model, which keeps the heating value of the product gas at the desired level in the presence of the matched disturbance: steam produced from water influx from surrounding aquifers and due to the moisture content of the coal.

Keywords:

Underground coal gasification (UCG), 1-D packed bed model, sequential

quadratic programming (SQP) and second order sliding mode control (SOSMC)

1. Introduction

Almost 84% of World's energy demand is fulfilled by the fossil fuels, of which share of coal is 28%, and in power generation it is the leading fuel [1]. Due to its relative abundance the coal is more likely to survive for a longer period of time as compared to oil and natural gas [2]. Due to the advent of clean coal technologies like Integrated Gasification Combined Cycle (IGCC), coal has become a clean source of electricity generation [3]. The IGCC systems generate electricity with higher efficiency than coal combustion based power plants, and high operating pressure in gasification process assists the separation of environmentally harmful contaminants from useful product gas [4, 5]. Coal can be gasified to produce synthesis gas or syngas: a mixture of CO, H_2, CH_4 and C_nH_m(higher hydrocarbons), either by gasification in specially designed surface gasifiers or gasifying the coal in-situ. UCG becomes the only choice for non-minable and very deep coal reservoirs [6].

UCG is a highly complex and nonlinear physicochemical process, though its concept is very simple and is elaborated in Fig 1. Two wells are drilled from surface to the coal seam. The oxidants are injected from the injection well after a permeable link is established between the wells. The inlet gas mixture includes air and H_2O (g) or O_2 and H_2O (g) or only air, which chemically reacts with already ignited coal to produce syngas, which is collected at the production well and can be used for power generation, industrial heating or as a chemical feedstock [6]. Three reaction zones are shown in the Fig 1,

which are in the order of decreasing temperature. The coal is initially dried and then pyrolysed to produce volatiles and char (a react able coal) in the pyrolysis and drying zone, from the heat produced by the oxidation reactions. The char oxidation and gasification reactions occur in the oxidation and gasification zones to produce the product gases, including the syngas.

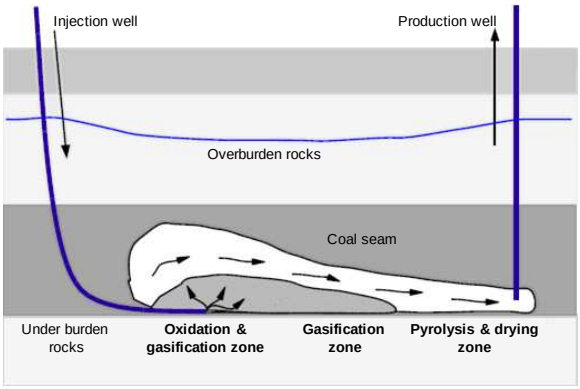

Figure 1: Concept of UCG [7]

Four different types of mathematical models of UCG are found in the literature: channel model [8], packed bed model [9, 10, 11, 12, 13], coal block model [14] and process model [15, 16, 17]. These models serve the following objectives: quantitative description of the process, evaluating a potential site for UCG and the study of various phenomena occurring within the UCG reactor. The models do not deal with the aspect of controlling the process, because even the complex 3-D models are far from being accurate. The inaccuracy in the models is mostly due to the uncertain in-situ environment and highly nonlinear nature of physical and chemical phenomena within the process.

The control of UCG is an emerging area of research and is so far limited to the laboratory scale UCG setups. Karol Kostur et al. [18, 19] im-

plemented proportional integral (PI) [20], and bang-bang and proportional summing (PS) type controllers respectively, for controlling important parameters of the lab scale UCG setup. However, the control of a real UCG process is a formidable job, especially considering the higher order dynamics, process non-linearities, uncertain in-situ environment and slowly varying disturbances. Therefore, a robust nonlinear control algorithm is of paramount importance in this scenario, one such algorithm is sliding mode control (SMC) which guards the closed loop system against parametric variations, effect of un-modeled dynamics and external disturbances [21, 22]. In our earlier work [23] a first order sliding mode control (FOSM) [24] was implemented on a simplified time domain model of UCG. The FOSM suffers from the problem of high frequency oscillations, formally called *chattering* in the control effort, which is normally due to the un-modeled dynamics [25], and it can cause wear and tear of the actuators. The algorithms that belong to the family of higher order sliding mode (HOSM) are very suitable for the control of the UCG process. Because, they utilize a reduced number of measured variables, converge to the reference in finite time, provide sufficient robustness against external disturbances, modeling uncertainties and parametric variations and also avoid chattering effects [26].

The current work is the extension of our previous work [27], focusing on the enhanced optimization and control of the UCG process model given in [27]. The objective of the optimization framework is to minimize the error between actual and experimental heating values of the product gas by optimizing ten variables (describing all the stoichiometry), as compared to the three variables in [27]. Now the optimization variables include all the input

parameters for balancing the chemical reactions (including coal composition parameters obtained from coal and char ultimate analysis) and steam to O_2 ratio at the *reaction front*. The reaction front is the highest temperature location along the length of the reactor, where the oxidation and gasification reactions take place. The choice of the variables caters for the uncertainty in coal and char ultimate analysis and in the amount of steam available for the gasification reactions. The molar fraction of the gases contributing to the heating value is highly dependent on the set of optimization variables. The data was collected from actual coal field, containing Lignite B coal (heating value less than 14.7 MJ/kg [28]). The distance between the injection and the production wells was 25 m, and the coal seam was 144m deep and 5m thick. It has been shown that the current optimization framework is superior to the previous case [27]. The super twisting, a HOSM control algorithm [29, 30] is also implemented on the model, which controls the heating value of the exit gas in the presence of a matched disturbance: steam generated by the water influx in to the UCG reactor. The super twisting algorithm provides necessary robustness along with reduced chattering.

2. UCG Reactor Model

The reactor model of UCG consists of eight gas species: CO, CO_2, H_2, H_2O, CH_4, N_2, O_2, and TAR (used to complete the stoichiometric balance of coal pyrolysis reaction) and two solid species: coal and char. The detailed description of the model is given in [27].

2.1. Mathematical Equations

The mathematical equations of the model consist of mass and energy conservation laws for both solid and gases, and conservation of momentum for the gases.

2.1.1. Solid phase equations

The mass balance for coal and char is given in Eq (1), where as Eq (2) represents the solid phase energy balance. Both of these equations are derived from laws of conservation of mass and energy for solids respectively.

$$\begin{aligned} \frac{\partial}{\partial t}\rho_i &= M_i \sum_{j=1}^{6} a_{s_{ij}} R_j \qquad (1) \\ where, & \\ \rho_i(0,x) &= \rho_{i_0}(x), \quad 0 \le x \le l \end{aligned}$$

$$\begin{aligned} \frac{\partial T_s}{\partial t} &= \frac{\frac{\partial}{\partial x}\left[(1-\phi)k\frac{\partial T_s}{\partial x}\right] + h(T-T_s) - H_s}{C_s} \qquad (2) \\ where, & \\ T_s(0,x) &= T_{s_0}(x), \quad 0 \le x \le l \\ \frac{\partial T_s}{\partial x}(t,0) &= \frac{\partial T_s}{\partial x}(t,l) = 0, \quad t \ge 0 \end{aligned}$$

where $\rho_i(t,x)$ is the density of ith solid (kg/m^3) in point (t,x), a_{sij} is the stoichiometric coefficient of solid i in reaction j, R_j is the rate of reaction j (mol/m^3/s), M_i is the molecular weight of solid component i (kg/mol), t is the variable for time (sec), x is the variable for length (m), $\rho_{i_0(x)}$ is the initial density of solid i, l is the length of the reactor (25 m), $T_s(t,x)$ is the

solid temperature (K) in point (t,x), $Ts_0(x)$ is the initial distribution of the solid temperature (K), T is the solid and gas temperature (K), ϕ is the coal bed porosity, k is the effective thermal conductivity of solids (J/m/s/K), h is the heat transfer coefficient (J/s/K/m^3), C_s is the total solid phase heat capacity (J/K/m^3), H_s is the solid phase heat source (J/s/m^3).

The equations for the reaction rates (R_j) are given in [27].

2.1.2. Gas phase equations

Eq (3) and (4) represent mass balance for all the gases and a combined gas phase energy balance respectively. Eq (5) and (6) shows how does pressure and velocity of gas mixture change as the function of the reactor's length, respectively. Eq (5) is called momentum balance equation and is derived from the law of conservation of momentum for the gas mixture.

$$\frac{dC_i}{dx} = \frac{1}{u_g}\left(-C_i\frac{du_g}{dx} + \sum_{j=1}^{6} a_{ij}R_j\right) \tag{3}$$

$$\frac{dT}{dx} = -\frac{1}{u_g C_g}\left[h\left(T - T_s\right) + H_g\right] \tag{4}$$

$$\frac{dP}{dx} = -\frac{u_g \mu}{2K} \tag{5}$$

$$\frac{du_g}{dx} = -\frac{u_g}{P}\frac{dP}{dx} + \frac{u_g}{T}\frac{dT}{dx} + \frac{RT}{P}\sum_{i=1}^{8}\sum_{j=1}^{6} a_{ij}R_j \tag{6}$$

where C_i is the concentration of ith gas (mol/m^3), u_g is the superficial gas velocity (m/s), $a_{ij}$is the stoichiometric coefficient of gas i in reaction j, C_g is the total gas phase heat capacity (J/K/m^3), H_g is the gas phase heat source (J/s/m^3), P is the gas pressure (Pa), K is the gas permeability coefficient (m^2), μ is the viscosity (Pa.s) and R is universal gas constant (m^3

Pa/mol/K).

The inlet boundary conditions for the gas phase Ordinary Differential Equations (ODEs) are given in Table 1

Table 1: Inlet boundary conditions for the gas phase equations

Sr	**Parameter**	**Value at $x = 0$**
1.	Inlet gas concentration	Mole percentage
	O_2	21%
	N_2	79%
	H_2O	0 in ignition and λC_{O_2} in gaisification
	Remaining gases	0
2.	T	T_0
3.	P	P_0
4.	u_g	G/C_{T_0}

where G is the flow rate of the injected air (moles/m^2/sec), $\lambda = \dfrac{C_{H_2O}}{C_{O_2}}$ is the steam to oxygen ration at $x = 0$, T_0 and P_0 are gas temperature and pressure at the inlet respectively, and C_{T_0} is the total concentration at $x = 0$.

2.2. Chemical kinetics and stoichiometry

It may be impossible to list all the chemical reactions defining the chemical kinetics of the UCG process, therefore for the sake of simplicity only six important chemical reactions are considered in the model, which are given in Table 2.

CH_aO_b and $CH_{\bar{a}}O_{\bar{b}}$ are empirical formulas for coal and char respectively. The values of a, b, $\bar{a}$, and $\bar{b}$ are determined by coal and char ultimate analysis. Reactions 2-5 are heterogeneous (char-gas) reactions where as reaction 6 is homogeneous (gas-gas) reaction. The coefficients ($a_{i,j}$ or $a_{s_{i,j}}$) are positive

Table 2: Chemical reactions considered in the model

Sr	Chemical equations
1.	**Pyrolysis**
	$CH_aO_b \rightarrow \lvert a_{s_{2,1}}\rvert CH_{\bar{a}}O_{\bar{b}} + \lvert a_{1,1}\rvert CO + \lvert a_{2,1}\rvert CO_2 + \lvert a_{3,1}\rvert H_2$ $+\lvert a_{4,1}\rvert H_2O + \lvert a_{5,1}\rvert CH_4 + \lvert a_{8,1}\rvert C_9H_c$
2.	**Char Oxidation**
	$CH_{\bar{a}}O_{\bar{b}} + \lvert a_{7,2}\rvert O_2 \rightarrow \lvert a_{2,2}\rvert CO_2 + \lvert a_{4,2}\rvert H_2O$
3.	**Steam gasification**
	$CH_{\bar{a}}O_{\bar{b}} + \lvert a_{4,3}\rvert H_2O \rightleftharpoons \lvert a_{1,3}\rvert CO + \lvert a_{3,3}\rvert H_2$
4.	**CO_2 gasification**
	$CH_{\bar{a}}O_{\bar{b}} + \lvert a_{2,4}\rvert CO_2 \rightleftharpoons \lvert a_{1,4}\rvert CO + \lvert a_{4,4}\rvert H_2O$
5.	**Methanation**
	$CH_{\bar{a}}O_{\bar{b}} + \lvert a_{3,5}\rvert H_2 \rightleftharpoons \lvert a_{1,5}\rvert CO + \lvert a_{5,5}\rvert CH_4$
6.	**Water gas shift reaction**
	$\lvert a_{1,6}\rvert CO + \lvert a_{4,6}\rvert H_2O \rightleftharpoons \lvert a_{2,6}\rvert CO_2 + \lvert a_{3,6}\rvert H_2$

for products and negative for reactants. The details of chemical reactions are presented in [27].

The stoichiometric coefficients are calculated in Eq (7) by using coal, char and TAR composition parameters [31].

Table 3: Input parameters for formulating stoichiometric coefficients

Sr	Parameter	Description
1.	a, b	Coal composition parameters
2.	$\bar{a}$, $\bar{b}$	Char composition parameters
3.	$a_{s_{2,1}}$	Moles of char per mole of coal
4.	$a_{3,1}$	Moles of H_2 per mole of coal
5.	$a_{5,1}$	Moles of CH_4 per mole of coal
6.	s	Atoms of C in coal which become atoms of C in TAR
7.	r	H to C ratio of TAR

$$
\begin{aligned}
|a_{4,1}| &= \frac{1}{2}\left(a - \bar{a}a_{s_{2,1}} - 2a_{3,1} - 4a_{5,1} - rs\right) \\
|a_{2,1}| &= b - 1 + a_{s_{2,1}}\left(1 - \bar{b}\right) - a_{4,1} + a_{5,1} + s \\
|a_{1,1}| &= 1 - a_{s_{2,1}} - a_{2,1} - a_{5,1} - s
\end{aligned} \tag{7}
$$

$$
\begin{aligned}
|a_{8,1}| &= \frac{s}{9} \\
|a_{4,2}| &= \frac{\bar{a}}{2} \quad = \quad |a_{4,4}| \\
|a_{7,2}| &= 1 + \frac{\bar{a}}{4} - \frac{\bar{b}}{2} \\
|a_{3,3}| &= 1 + \frac{\bar{a}}{2} - \bar{b} \quad = \quad |a_{2,4}| \\
|a_{4,3}| &= 1 - \bar{b} \quad = \quad |a_{5,5}| \\
|a_{1,4}| &= 2 + \frac{\bar{a}}{2} - \bar{b} \\
|a_{3,5}| &= 2 - \frac{\bar{a}}{2} - 2\bar{b} \\
|a_{1,5}| &= \bar{b}
\end{aligned}
$$

All the other coefficients in Table 2 have a unity magnitude.

2.3. Solution of the UCG reactor model

The mathematical model consists of two sets of equations: eleven first order gas phase ODEs in length and three solid phase partial differential equations (PDEs) in time and length. The gas phase ODEs being stiff in nature are simultaneously solved as a boundary value problem using TR-BDF2, an implicit Runge-Kutta algorithm [32]. The boundary conditions for the gas phase system are set by the flow rate of injected air, steam concentration

near the reaction front and the inlet gas temperature and pressure. The inlet gases remain unreacted until they approach the reaction front. Therefore, conceptually the inlet well/boundary and the reaction front refer to the same location along the length of the UCG reactor, i.e., $x = 0$. The solid phase equations are first discretized [27] and then solved for new time. The solid phase equations are discretized with the step size of 20 secs Eq (1) is discretized using forward Euler method, and the explicit finite difference technique is used to discretize Eq (2). For initializing the solid phase system, the initial densities of coal and char $\boldsymbol{\rho_{i_0}(x)}$, and ignition temperature profile $\boldsymbol{T_{s_0}(x)}$ are incorporated in the model.

The complete solution strategy is summarized in Table 4. The solution starts by initializing the values of coal parameters and then generating the initial conditions for solid and gas phase systems respectively. When the solution progresses in time the solid phase system is updated first, and then the gas phase system is advanced in time using the updated solution of the solid phase system. The solution of the mathematical model evolves in both time and space. The change with time is brought by the solid phase system, where as the change in length domain is caused by the gas equations.

The model is simulated in the ignition phase for first 1000 s and afterwards in the gasification mode. The ignition phase acts as the initial condition for the gasification phase. During ignition coal bed is heated to pyrolyze the coal in to char, and to achieve a sufficient temperature for subsequent gasification reactions. During gasification mode the water is allowed to enter the UCG reactor, which converts in to steam due to the high temperature and pressure of the cavity. The concentration of the steam produced by the water influx

Table 4: Summary of solution procedure to solve the reactor model

1.	input all the coal properties and operating conditions
2.	initialize solid phase system (Eqs (1) and (2))
	• $\boldsymbol{\rho_i(0,x) = \rho_{i_0}(x)}$ and $\boldsymbol{T_s(0,x) = T_{s_0}(x)}$
3.	initialize gas phase system
	• simultaneously solve Eqs (3), (4), (5) and (6) as a boundary value problem by TR-BDF2 algorithm [32], to yield $\boldsymbol{Y_{gas}{}^{*}(0,x)}$
4.	iterative loop
	• solve discrete solid phase equations by using $\boldsymbol{R_j(t,x)}$ to yield $\boldsymbol{\rho_i(t+dt,x)}$ and $\boldsymbol{T_s(t+dt,x)}$
	• solve gas phase system with $\boldsymbol{R_j(t+dt,x)}$ by repeating procedure in step 3 to get $\boldsymbol{Y_{gas}(t+dt,x)}$
5.	update time, $t^{n+1} = t^n + dt$
6.	stop if simulations ends, else go to step 4

*solution of Eqs (3), (4), (5) and (6)

and the moisture content in the coal, sets the boundary condition for the mass balance of steam and assists the gasification reactions and hence the production of syngas. The amount of water influx in to the UCG reactor can be controlled by varying the pressure in the reactor [33].

3. Model Validation

3.1. Experimental Setup

The experimental setup for the UCG process is shown in Fig 2. Two types of compressors are used to supply compressed air during the UCG field trials. The SIAD TEMPO^2 1500 high pressure (HP) compressors (Fig 3) are used during link establishment via reverse combustion linkage [34] and the Atlas Copco GA 250 low pressure (LP) compressors (Fig 4) are used during

gasification process. After link establishment, the LP compressor/s send air to the control room, where its flow rate is manipulated by the control valve, either manually or by the programmable logic controller (PLC). The air at specific flow rate is delivered to the injection well, where it chemically reacts with the already ignited coal seam. The product gases are retrieved from the outlet well. For a single gasifier, a network of two pipes is essential, one for supplying compressed air to the coal seam and the other for transporting output gases to the gas analyzer. The UCG field used for the current experiment is shown in Fig 5. The blue pipes carry compressed air and product gases are contained in the red pipes. The GAS 3100 R coal gas/syngas analyzer (Fig 6) measures the molar fractions of all the gases [35]. The molar fractions of CO, CO_2, CH_4 and C_nH_m are measured by dual beam non dispersive infra red (NDIR) detectors. The thermal conductivity (TCD) detector and galvanic fuel cell are used to measure molar fractions of H_2, and O_2 respectively. The heating value of the exit gas is calculated by the following relationship.

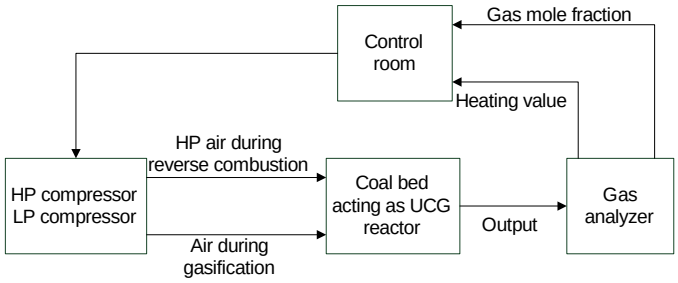

Figure 2: Block diagram of the UCG setup

$$HV_{exp} = m_{CO_{exp}} H_{CO} + m_{C_nH_{m_{exp}}} H_{C_nH_m} + m_{CH_{4exp}} H_{CH_4} + m_{H_{2exp}} H_{H_2} \quad (8)$$

where HV_{exp} is the experimental heating value of the exit gases (KJ/m^3),

Figure 3: SIAD TEMPO^2 1500 high pressure compressors

Figure 4: Atlas Copco GA 250 low pressure compressor

and $m_{i_{exp}}$ and H_i are the experimental percentage mole fraction and heat of combustion (KJ/m^3) of gas component i respectively. The analyzer is integrated on line, the steam is removed from the gas mixture and the mole fraction of remaining gases is measured. The measurements show that there are only traces of higher hydrocarbons C_nH_m

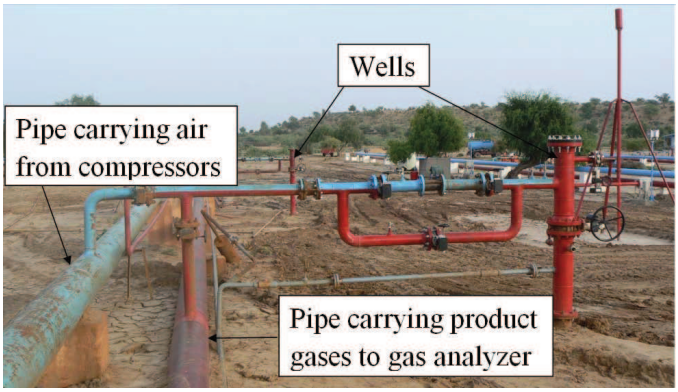

Figure 5: UCG field

Figure 6: GAS 3100 R coal gas/syngas analyzer

3.2. Optimization

3.2.1. Problem Statement

The following constrained nonlinear optimization (nonlinear programing) problem is formulated to address the uncertainty in ultimate analysis of coal

and char, and in steam to oxygen ratio at the reaction front λ, an important operating condition for the UCG process.

$$min_x f(x),\ such\ that \begin{cases} \boldsymbol{c(x)} & \leq \boldsymbol{0} \\ \boldsymbol{Ax} & \leq \boldsymbol{b} \\ \boldsymbol{lb} & \leq \boldsymbol{x} \leq \boldsymbol{ub} \end{cases} \tag{9}$$

where $\boldsymbol{x} \in \Re^n$ is a vector of n optimization variables, $f : \Re^n \rightarrow \Re$ is the objective function to be minimized, $\boldsymbol{c} : \Re^n \rightarrow \Re^m$ is a function which returns a vector of m nonlinear inequality constraints, $\boldsymbol{A} \in \Re^{p \times n}$ and $\boldsymbol{b} \in \Re^p$ represent p linear inequality constraints, and $\boldsymbol{lb}$ and $\boldsymbol{ub}$ are lower and upper bounds on the optimization variables respectively.

3.2.2. Optimization variables and objective function

The optimization variables and objective function are given in Eq (10) and (11) respectively. The optimization variables include all the parameters already presented in Table 3 and the parameter λ. The uncertainty in the coal and char composition parameters also affects the other input parameters for computing stoichiometric coefficients for the chemical reactions. The steam to oxygen ratio λ is very critical in the formation of syngas [12, 31]. As discussed earlier in Section 2.3 that the steam participating in the gasification reactions is produced by the moisture content in the coal and water influx from the surrounding aquifers. The latter can be controlled by the varying the operating pressure of the reactor, but there is no mechanism to measure the exact amount of steam at the reaction front. Therefore λ is optimized in order to compensate for the uncertainty in the steam available for the

gasification reactions. All the optimization variables effect the composition and heating value of the product gas. The objective function is the sum of the squares of the relative error of the experimental and simulated heating values at each time instant.

$$
\begin{aligned}
\boldsymbol{x^T} &= \begin{bmatrix} a & b & \bar{a} & \bar{b} & \lambda & r & s & a_{3,1} & a_{5,1} & a_{s_{2,1}} \end{bmatrix} && (10)\\
f &= \left\| \boldsymbol{e}\left(\boldsymbol{t}\right) \right\|_2^2 && (11)\\
\boldsymbol{e}\left(\boldsymbol{t}\right) &= \frac{\boldsymbol{HV_l}\left(\boldsymbol{t}\right) - \boldsymbol{HV_{exp}}\left(\boldsymbol{t}\right)}{\boldsymbol{HV_{exp}}\left(\boldsymbol{t}\right)} \\
HV_l &= m_{CO,l}H_{CO} + m_{C_nH_{m,l}}H_{C_nH_m} + m_{CH_4,l}H_{CH_4} + m_{H_{2,l}}H_{H_2} \\
m_{C_i} &= 100 \times \frac{C_i}{\tilde{C_T}} \\
\tilde{C_T} &= \sum_{i=1, i\neq 4}^{8} C_i
\end{aligned}
$$

where HV is simulated heating value, m_{C_i} is the percentage mole fraction of a gas i, $\tilde{C_T}$ (moles/m^3) is total concentration of the gases without steam and the subscript l indicates the value at $x = l$

The solution of the mathematical model does not yield mole fraction of the higher hydrocarbons C_nH_m separately, but they contribute in the mole fraction of TAR.

3.2.3. Constraints

There are seven linear ($p = 7$) and three nonlinear ($m = 3$) inequality constraints in the optimization framework. The linear constraints are given in Eq. (12). First four constraints satisfy the relationship between coal and char composition parameters ($0.02a \leq \bar{a} \leq 0.2a$ and $0.02b \leq \bar{b} \leq 0.2b$), and

the last three ensure that the magnitudes of all stoichiometric coefficients in reactions 2-5 in Table. 2 are positive.

$$\begin{aligned} -0.2x_1 + x_3 &\leq 0 \\ 0.02x_1 - x_3 &\leq 0 \\ -0.2x_2 + x_4 &\leq 0 \\ 0.02x_2 - x_4 &\leq 0 \\ -0.5x_3 + x_4 &\leq 1 \\ 0.25x_3 + x_4 &\leq 1 \\ x_4 &\leq 1 \end{aligned} \tag{12}$$

The matrix $\boldsymbol{A}$ and vector $\boldsymbol{b}$ in Eq. (9) can be written from the Eq. (12)

$$\begin{aligned} \boldsymbol{A^T} &= \begin{bmatrix} -0.2 & 0.02 & 0 & 0 & 0 & 0 & 0 \\ 0 & 0 & -0.2 & 0.02 & 0 & 0 & 0 \\ 1 & -1 & 0 & 0 & -0.5 & 0.25 & 0 \\ 0 & 0 & 1 & -1 & 1 & 1 & 1 \\ 0 & 0 & 0 & 0 & 0 & 0 & 0 \\ 0 & 0 & 0 & 0 & 0 & 0 & 0 \\ 0 & 0 & 0 & 0 & 0 & 0 & 0 \\ 0 & 0 & 0 & 0 & 0 & 0 & 0 \\ 0 & 0 & 0 & 0 & 0 & 0 & 0 \\ 0 & 0 & 0 & 0 & 0 & 0 & 0 \end{bmatrix} \\ \boldsymbol{b^T} &= \begin{bmatrix} 1 & 1 & 1 & 0 & 0 & 0 & 0 \end{bmatrix} \end{aligned} \tag{13}$$

The nonlinear constraints in Eq. (14) ensure the magnitudes of the stoichiometric coefficients of CO , CO_2 and H_2O in coal pyrolysis reaction stay positive respectively.

Therefore all the constraints make sure that the magnitudes of all the stoichiometric coefficients in the chemical reactions are positive, and all the chemical reactions are properly balanced.

$$\begin{aligned}
&\frac{1}{2}x_1 - x_2 - x_8 - 3x_9 - \frac{1}{2}x_7\,(x_6 + 2) + \frac{1}{2}x_{10}\,(2x_4 - x_3 - 2) + 1 < 0 \\
&-\frac{1}{2}x_1 + x_2 + x_8 + 4x_9 + \frac{1}{2}x_7\,(x_6 + 4) + \frac{1}{2}x_{10}\,(4 - 2x_4 + x_3) - 2 < 0 \\
&-x_1 + x_3x_{10} + 2x_8 + 4x_9 + x_6x_7 < 0
\end{aligned} \tag{14}$$

3.2.4. Solution of optimization problem

The constrained nonlinear optimization problem in Eq (9) is solved by Matlab function *fmincon*, using the SQP algorithm. The SQP is the most successful method for solving such problems. In this method the nonlinear program in Eq (9) is approximated by a quadratic programming (QP) subproblem at the current estimate, and then the QP is solved to generate a better approximation of the next estimate. In this way the nonlinear program is converted in to a sequence of QP subproblems, which are iteratively solved to reach the solution [36]. The UCG reactor model is solved using the procedure elaborated in Table 4 before computing the objective function in Eq (11).

The confidence intervals of the optimization variables are also calculated in order to validate the robustness of there estimates. The optimization problem is solved for eleven different data sets and then *95% confidence*

interval for the estimates of the variables is calculated (Eq (15)) by using the method given in [37]. The error statistics for the optimization variables is given in Table 5

$$\theta \quad = \quad \hat{\theta} \pm t_{tab} \frac{s}{\sqrt{n}} \tag{15}$$

where θ is the true value (mean of large set of replicates), $\hat{\theta}$ is the mean of sub samples, $n = 11$ is the number of sub samples. $t_{tab} = 2.228$ (taken from the two sided t-table [37] against $df = n - 1 = 10$) is the statistical value for 95% confidence and s is the standard deviation of mean of sub samples.

Table 5: Optimization variables and there error bounds

Sr	**Parameter**	**Value**	**Error bounds at 95% confidence interval**
1.	a	0.8543	± 0.0266
2.	b	0.1985	± 0.0062
3.	$\bar{a}$	0.0825	± 0.0014
4.	$\bar{b}$	0.0152	± 0.0008
5.	λ	2.0597	± 0.0646
6.	r	2.7514	± 0.0378
7.	s	0.1299	± 0.0099
8.	a_{31}	0.0824	± 0.0002
9.	a_{51}	0.0304	± 0.0044
10.	$a_{s_{21}}$	0.7739	± 0.0181

3.3. Result Comparison

The simulated and experimental results for three different data sets are compared for the heating value and molar fractions of CO, H_2 and Ch_4 (Fig 7). In order to show the improvement in the model validation, the

results of the current (Case a: optimization using ten variables) and previous (Case b: optimization using three variables [27]) optimization techniques are also compared

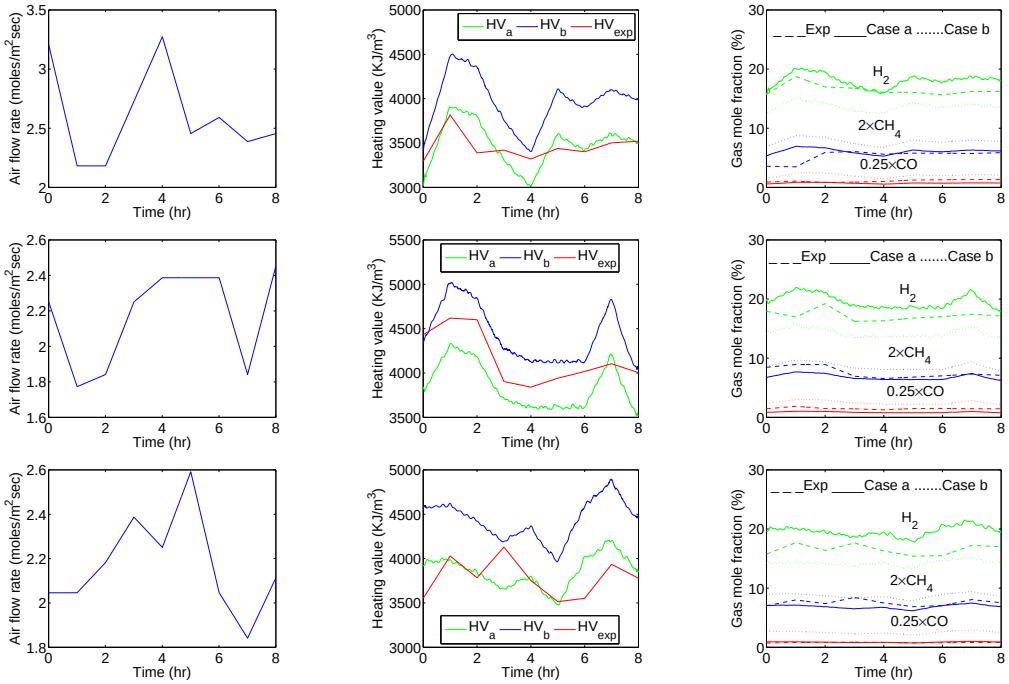

Figure 7: Comparison between experimental and simulated results for three different data sets using both optimization cases (Case a: optimization using ten variables and Case b: optimization using three variables)

Table 6 shows the relative errors (Eq (16)) of experimental and simulated results for both cases.

$$\|\boldsymbol{e_{rel}}\|_2 = \frac{\|\hat{\boldsymbol{y}} - \boldsymbol{y}\|_2}{\|\boldsymbol{y}\|_2} \tag{16}$$

where $\boldsymbol{e_{rel}}$ is the relative error of experimental ($\boldsymbol{y}$) and simulated parameter ($\hat{\boldsymbol{y}}$).

Table 6: Relative error for experimental and simulated results of different parameters

	% Relative error (Case a)			% Relative error (Case b)		
Parameter	**data 1**	**data 2**	**data 3**	**data 1**	**data 2**	**data 3**
HV	4.81	7.93	5.96	15.92	7.55	18.07
m_{CO}	37.53	41.59	13.36	89.65	69.5	214.98
m_{H_2}	10.83	14.95	19.16	17.69	17.25	14.80
m_{CH_4}	23.40	11.35	10.95	48.44	15.71	16.17

The results in the Table 6 show that the results of Case a are better than those of Case b. It can also be seen that the relative error in case of the gas mole fractions is higher than that of the heating value, which is due to the choice of the objective function (Eq (11)). The control of UCG process in Section 4 requires the measurement of the heating value only, therefore, the deviation in the molar fractions of the gases is not very critical for the UCG control system.

4. Controller Design

4.1. Control problem

As discussed in Section 2.3 and [27] that the optimum value of steam at the reaction front is necessary for a successful UCG process, but if its value increases or decreases beyond the optimal value it can either decrease the overall temperature of the reactor or reduce the production of syngas by minimizing the magnitude of steam gasification reaction. The total amount of steam at the reaction front is produced from moisture content in the coal and

due to the water influx from surrounding aquifers, the latter can be controlled by maintaining a pressure gradient in the UCG reactor. The concentration of the steam can vary during the gasification process. The steam concentration at the reaction front is mostly dependent upon the flow rate of the steam generated by the water influx. As the control input $u(t)$ (flow rate of injected air, G in Table 1) also acts at the reaction front, therefore, the steam flow rate at the reaction front is the matched, but bounded disturbance $\delta(t)$ ($\left\|\delta\left(t\right)\right\| \leq \delta_0 > 0$). The boundary conditions for the concentration of O_2, N_2 and H_2O (Eq (3)) are set by $u(t)$ and $\delta(t)$ respectively. Therefore, the control problem is to maintain a desired heating value of the product gas at the outlet ($x = l$) in the presence of $\delta(t)$.

4.2. State space representation of the UCG process at the outlet

The finite dimensional state space of the single input single output UCG process at the outlet $x = l$ is given as:

$$
\begin{aligned}
\dot{\boldsymbol{z}}(\boldsymbol{t}) &= \boldsymbol{f}(\boldsymbol{z},\boldsymbol{t}) + \boldsymbol{g}(\boldsymbol{z},\boldsymbol{t})\,\boldsymbol{u}(\boldsymbol{t}) + \boldsymbol{d}(\boldsymbol{z},\boldsymbol{t})\,\boldsymbol{\delta}(\boldsymbol{t}) \qquad (17)\\
HV_l(t) &= w(z,t)\\
&where,\\
\boldsymbol{z}^T &= \begin{bmatrix}\rho_1 & \rho_2 & T_s\end{bmatrix}\\
\boldsymbol{f} &= \begin{bmatrix} -M_1 R_1(z) \\ a_{s_{2,1}} M_2 R_1(z) \\ \dfrac{1}{C_s(z)}\left[h\exp\left(-\dfrac{h}{vC_g}l\right)[T_0 - z_3] - \Delta H_1 R_1(z)\right]\end{bmatrix}\\
\boldsymbol{g}^T &= 0.21\exp(-\eta(z)\,l) C R_2(z)\begin{bmatrix}0 & -M_2 & -\dfrac{\Delta H_2}{C_s(z)}\end{bmatrix}\\
\boldsymbol{d}^T &= C R_3(z)\begin{bmatrix}0 & -M_2 & -\dfrac{\Delta H_3}{C_s(z)}\end{bmatrix}\\
w &= \frac{100}{\tilde{C}_T}\left[A_1\int_0^l R_1(z)\,dx + A_2\int_0^l R_3(z)\,dx\right]
\end{aligned}
$$

where the system state vector is $\boldsymbol{z} \in \boldsymbol{\Re^3}$, $\boldsymbol{f} \in \boldsymbol{\Re^3}$ is the nonlinear function of states, $\boldsymbol{g} \in \boldsymbol{\Re^3}$ is the input vector, $\boldsymbol{d} \in \boldsymbol{\Re^3}$ is the disturbance vector, u, d and HV_l are scalar input, disturbance and the output (heating value at the outlet) respectively and w is the nonlinear function of states representing the output. The complete derivation of the state space is given in Appendix A

4.3. Super twisting sliding mode controller

The controller is situated in the control room of the UCG setup (Fig. 2). For simulations the dynamics of the compressor and the gas analyzer are ignored. The simplified block diagram of the UCG control system is shown in Fig. 8. The output from the UCG reactor model is fed back in to the

controller which compares it with the desired value and based on the super twisting control algorithm computes the flow rate of the injected air.

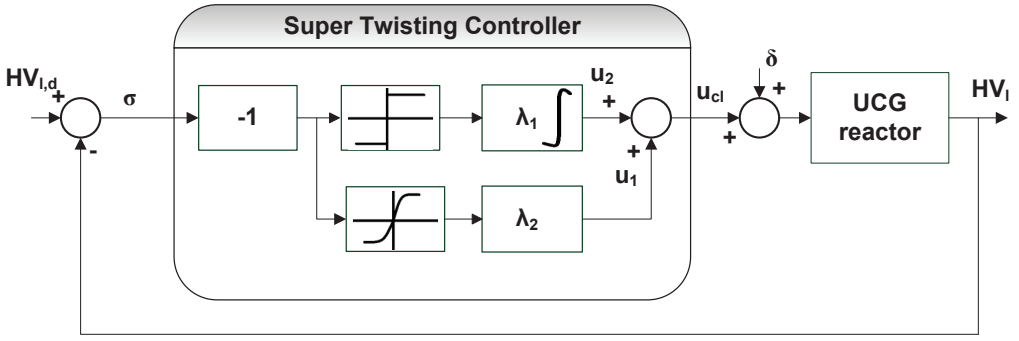

Figure 8: Block diagram of the closed loop system with super twisting algorithm

The super twisting controller is used because the output to be controlled has a relative degree one with respect to the control input. This control algorithm has following remarkable advantages: the output attains its desired value in finite time, the control input is a continuous function of states, it does not require the derivative of the output and it has the ability to reject the unknown bounded disturbance [30, 38]. The super twisting is a second order sliding mode as the sliding occurs in the manifold $\dot{\sigma} = \sigma = 0$.

Consider the sliding variable and its dynamics.

$$\begin{aligned} \sigma &= HV_{l,d} - HV_l \\ \ddot{\sigma} &= \phi(t,x,u) + \psi(t,x,u)\,\dot{u}(t) \end{aligned} \tag{18}$$

where $\sigma \in \Re$ is sliding surface, which is the error between desired ($HV_{l,d}$) and actual (HV_l) heating values at the outlet. The bounds on the functions ϕ and ψ are: $|\phi| \leq \Phi$ and $0 \leq \Psi_m \leq \psi(\sigma,t) \leq \Psi_M$ respectively, with $\Phi,\ \Psi_m,\ \Psi_M \in \Re^+$.

Then the super twisting based control law can be given as a sum of two components

$$\begin{aligned} u_{cl} &= u_1 + u_2 \\ u_1 &= \begin{cases} -\kappa_1 |\sigma_0|^{0.5} sgn(\sigma), & if |\sigma| > |\sigma_0| \\ -\kappa_1 |\sigma|^{0.5} sgn(\sigma), & if |\sigma| \leq |\sigma_0| \end{cases} \\ \dot{u}_2 &= \begin{cases} -\kappa_2 sgn(\sigma), & if |u| \leq 1 \\ -u, & if |u| > 1 \end{cases} \end{aligned} \tag{19}$$

where $u_{cl} \in \Re$ is the closed loop control input. The values of the constants κ_1 and κ_2 should satisfy

$$\begin{aligned} \kappa_1^2 &\geq \frac{4\Phi}{\Psi_m^2} \frac{\Psi_M (\kappa_2 + \Phi)}{\Psi_m (\kappa_2 - \Phi)} \\ \kappa_2 &> \frac{\Phi}{\Psi_m} \end{aligned} \tag{20}$$

If the controller gains κ_1 and κ_2 satisfy the above conditions then the system output converges to the desired value in finite time.

The UCG process is operated in the closed loop after the process is settled in the gasification phase. The input u to the UCG process is given by.

$$\begin{aligned} u(t) &= \begin{cases} G & t \leq t_{ol} \\ \theta u_{cl} + (1-\theta) G & t_{ol} < t < t_{cl} \\ u_{cl} & t \geq t_{cl} \end{cases} \\ \theta &= \frac{(t - t_{ol})}{(t_{cl} - t_{ol})}, \quad 0 < \theta < 1 \end{aligned} \tag{21}$$

UCG process is operated in open loop till t_{ol} (open loop time), and the operation is closed loop from t_{cl} (close loop time). For simulation $t_{ol} = 2hrs$ and $t_{cl} = 4hrs$, and the sample period $T = 2secs$ is chosen for the implementation of the controller . A convex set (C) is formed by u [39] for interval $t_{ol} < t < t_{cl}$

$$u_{cl},\, G \in C \Longrightarrow \theta u_{cl} + (1-\theta)\, G \in C$$

which ensures the smooth transition from open loop to closed loop operation of the process.

The simplified state space representation of the UCG process in Eq (17) is only used to select the values of the controller gains (κ_1 and κ_2) from the conditions in Eq (20). In order to justify the simplifications, the synthesized controller is implemented on the actual UCG reactor model in Section 2.

4.4. Results and discussion

Fig 9 shows the control input, the regions Ω_1 and Ω_3 represent open loop and closed loop inputs respectively, where as Ω_2 is the region of transition from open loop to closed loop. The profile of steam flowrate at the reaction front is shown in Fig 10. For simulations the concentration of the steam at $x = 0$ is $C_{H_2O} = \frac{\delta}{v}$ (this boundary condition for the mass balance of steam is used in the closed loop system). As discussed in [27], the process of UCG is dominated by three chemical reactions: coal pyrolysis, char oxidation and steam gasification. The latter two reactions occur at the reaction front, and produce CO_2 and syngas respectively. Along with the dependence on temperature, the char oxidation reaction is highly dependent on the mole fraction of O_2, where as steam gasification reaction requires steam to occur.

Therefore, when the concentration of steam increases, it tires to increase the production of syngas and hence the HV_l. The controller reacts to the situation by injecting more O_2 in the reactor to produce CO_2, which balances the increase in mole fraction of CO and H_2 in order to keep HV_l at the desired level. Similarly the controller reduces the amount of O_2, when the steam concentration is decreased. This effect can be witnessed in Figs 9 and 10.

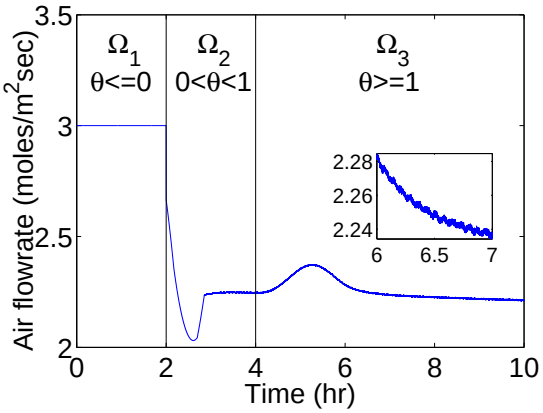

Figure 9: Control effort u (zoomed view showing the chattering phenomenon).

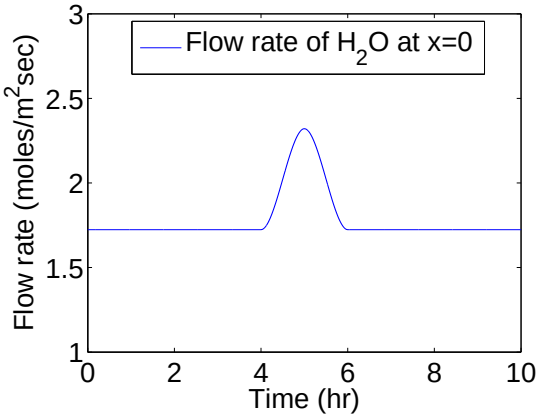

Figure 10: Input disturbance δ.

The desired and actual heating values of the product gas are shown in

Fig 11, and their difference (sliding surface) is shown in Fig 12. It can be seen from the figures that the control algorithm successfully keeps the heating value at a desired level in the presence of matched disturbance, with satisfactory performance. During the simulation it has been observed that there is a trade off between the speed and smoothness of the response, if $t_{cl} - t_{ol}$ is small then HV_l has higher percentage overshoot but it settles quickly and vice versa. UCG is a slow process, therefore, the selected values of t_{cl}, t_{ol} ensure that HV_l settles in less than $1hr$ with overshoot of 8.04%.

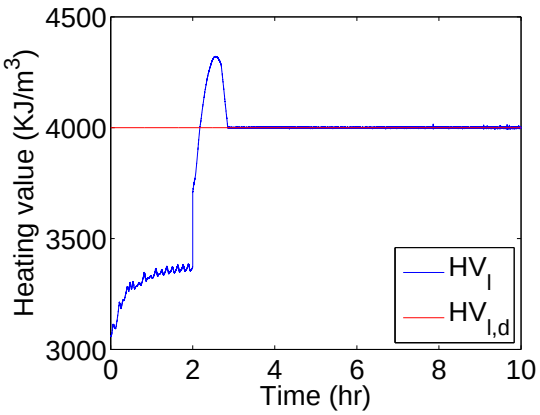

Figure 11: Desired and actual heating values at the outlet.

5. Conclusion

It has been shown that the actual process of UCG can be successfully modeled by the 1-D packed bed modeling technique. The uncertainties in coal and char ultimate analyses, and steam to oxygen ratio at the inlet well are catered by formulating a nonlinear optimization problem. The optimization problem is solved by using SQP algorithm, and the results of the solved modeled are validated by comparison with the actual field trials. The results

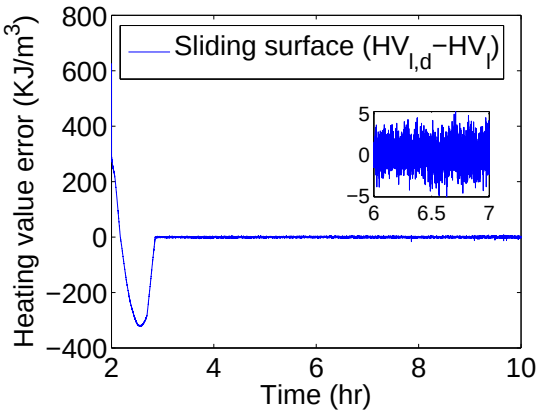

Figure 12: Sliding surface σ (zoomed view showing the chattering phenomenon).

for the molar fraction of gases can be improved by formulating a multi-objective optimization problem.

It has been further shown that the UCG process with huge nonlinearities, uncertainties and external disturbance can be successfully controlled by a robust super twisting SMC algorithm. The simulation results show that the controller maintains the desired heating value of the exit gas in finite time by nullifying the effect of variations in the flow rate of the water influx.

Acknowledgements

Authors would like to acknowledge the National ICT R&D Fund for providing financial support under the grant No.ICTRDF/TR&D/2011/14. The authors are also grateful to the UCG project Thar for providing access to the UCG site and other technical and financial assistance for the completion of the research work. The contribution of the Control And Signal Processing Research (CASPR) group at Muhammad Ali Jinnah University is also appreciated.

Appendix A. Infinite dimensional state space of the UCG process

The partial differential equations describing the mass and energy balances of the solid phase system in Section 2.1.1 and the heating value of the gases constitute the infinite dimensional state space of the UCG reactor model. In an infinite dimensional system, the solution evolves on an infinite dimensional Hilbert space [40].

The process of UCG is dominated by the three reactions: Coal pyrolysis, char oxidation and steam gasification [12, 27], therefore, only these reactions are considered here. The three states of the reactor model are:

$$
\begin{aligned}
\dot{\rho_1}(t,x) &= -M_1 R_1(t,x) \qquad (A.1)\\
\dot{\rho_2}(t,x) &= M_2\left[a_{s_{2,1}} R_1(t,x) - R_2(t,x) - R_3(t,x)\right]\\
\dot{T_s}(t,x) &= \frac{1}{C_s(t,x)}\left[B T_s''(t,x) + h\left(T(x) - T_s(t,x)\right) - H_s(t,x)\right]\\
&where\\
T(x) &= T_0 \exp\left(-\frac{h}{vC_g}x\right) + T_s\left[1 - \exp\left(-\frac{h}{vC_g}x\right)\right]\\
C_s(t,x) &= \rho_1(t,x)\, c_{s_1} + \rho_2(t,x)\, c_{s_2}\\
H_s &= \Delta H_1 R_1(t,x) + \Delta H_2 R_2(t,x) + \Delta H_3 R_3(t,x)
\end{aligned}
$$

where $B = (1-\phi)k$, h, C_g and v(superficial gas velocity) are considered as constants, ΔH_i is the heat of the reaction i (J/sec/m^3) and c_{s_i} represent the heat capacity of coal and char (J/g/K) respectively. T is the solution of Eq (4), with $T(0) = T_0$ and it also assumes that the pressure of the gas phase is constant. If a well linked channel is established between inlet and outlet wells, then the pressure of the gas does not drop significantly through the UCG reactor. The expressions for rates are given below:

$$
\begin{aligned}
R_1 &= 5\frac{\rho_1}{M_1}\exp\left(\frac{-6039}{T_s}\right) \\
R_2 &= C_7 C R_2 \\
CR_2 &= \frac{9.55\times 10^8 \rho_2 P \exp\left(\dfrac{-22142}{T_s}\right) k_y}{C_T\left[M_2 k_y\sqrt{T_s} + 9.55\times 10^8 \rho_2 P \exp\left(\dfrac{-22142}{T_s}\right)\right]} \\
C_7 &= 0.21u\left(t\right)\exp\left(-\eta x\right) \\
\eta &= \frac{|a_{7,2}|}{v}\int_0^x CR_2\, dx
\end{aligned}
\tag{A.2}
$$

$$
\begin{aligned}
R_3 &= \delta\left(t\right) CR_3 \\
CR_3 &= \frac{k_y P^2 \rho_2 \exp\left(5.052 - \dfrac{12908}{T_s}\right)}{C_T v\left[P^2\exp\left(5.052-\dfrac{12908}{T_s}\right)\rho_2 + k_y M_2\left(P+\exp\left(-22.216+\dfrac{24880}{T_s}\right)\right)^2\right]}
\end{aligned}
$$

where $k_y = 0.1h$, and C_T (total concentration of all the gases) are constants. C_7 is the solution of the mass balance of O_2 (Eq (3)) with $C_7(0) = 0.21u$.

Heating value of the gases is the output of the UCG reactor model, which is a function of system states.

$$
HV\left(x\right) = \frac{100}{\tilde{C_T}}\left[H_1 C_1\left(x\right) + H_3 C_3\left(x\right) + H_5 C_5\left(x\right) + H_8 C_8\left(x\right)\right] \tag{A.3}
$$

where $HV\left(x\right)$ is the distributed heating value, $\tilde{C_T}$ the total concentration of all the gases excluding steam is assumed to be constant, C_i and H_i are the

concentration and heat of combustion of gas i and $i = 1, 3, 5, 8$ represents CO, H_2, CH_4 and C_nH_m respectively.

Eq (A.3) can be solved for $HV(x)$ by solving Eq (3) as a boundary value problem for C_1, C_3, C_5 and C_8 with $C_i(x = 0) = 0$, the particular solution for C_i is given as:

$$\begin{aligned} C_i(x) &= \zeta_i \qquad (A.4) \\ where, & \\ \zeta_i &= \frac{1}{v}\sum_{j=1}^{3} a_{i,j}\int_0^x R_j\,dx \end{aligned}$$

Now the solution of Eq (A.3) can be written as

$$\begin{aligned} HV(t,x) &= \frac{100}{\tilde{C_T}}\left[A_1\int_0^x R_1\,dx + A_3\int_0^x R_3\,dx\right] \qquad (A.5) \\ where, & \\ A_1 &= a_{1,1}H_1 + a_{3,1}H_3 + a_{5,1}H_5 + a_{8,1}H_8 \\ A_3 &= a_{1,3}H_1 + a_{3,3}H_3 \end{aligned}$$

The finite dimensional state space (Eq (17)) is obtained by substituting $x = l$.

References

[1] B. Bose, Global energy scenario and impact of power electronics in 21st century, Industrial Electronics, IEEE Transactions on 60 (2013) 2638–2651.

[2] G. Maggio, G. Cacciola, When will oil, natural gas, and coal peak?, Fuel 98 (2012) 111 – 123.

[3] A. Khadse, M. Qayyumi, S. Mahajani, P. Aghalayam, Underground coal gasification: A new clean coal utilization technique for India, Energy 32 (2007) 2061 – 2071.

[4] C. Descamps, C. Bouallou, M. Kanniche, Efficiency of an integrated gasification combined cycle IGCC power plant including CO_2 removal, Energy 33 (2008) 874 – 881.

[5] N. V. Gnanapragasam, B. V. Reddy, M. A. Rosen, Hydrogen production from coal gasification for effective downstream CO_2 capture, International Journal of Hydrogen Energy 35 (2010) 4933 – 4943.

[6] A. W. Bhutto, A. A. Bazmi, G. Zahedi, Underground coal gasification: From fundamentals to applications, Progress in Energy and Combustion Science 39 (2013) 189 – 214.

[7] G. Perkins, V. Sahajwalla, Modelling of heat and mass transport phenomena and chemical reaction in underground coal gasification, Chemical Engineering Research and Design 85 (2007) 329 – 343.

[8] C. Magnani, S. Farouq Ali, A two-dimensional mathematical model of the underground coal gasification process, in: Fall Meeting of the Society of Petroleum Engineers of AIME, 1975.

[9] R. D. Gunn, D. L. Whitman, An in situ coal gasification model (forward mode) for feseability studies and design, Report of investigations, Laramie Energy Research Center, Laramie, Wyoming, 1976.

[10] A. Winslow, Numerical model of coal gasification in a packed bed, Symposium (International) on Combustion 16 (1977) 503 – 513.

[11] C. B. Thorsness, R. B. Rozsa, Insitu coal-gasification: Model calculations and laboratory experiments, Society of Petroleum Engineers Journal 18 (1978) 105–116.

[12] A. Khadse, M. Qayyumi, S. Mahajani, Reactor model for the underground coal gasification UCG channel, International Journal of Chemical Reactor Engineering 4 (2006).

[13] M. Seifi, J. Abedi, Z. Chen, Application of porous medium approach to simulate UCG process, Fuel 116 (2014) 191 – 200.

[14] G. Perkins, V. Sahajwalla, Steady-state model for estimating gas production from underground coal gasification, Energy & Fuels 22 (2008) 3902–3914.

[15] E. N. J. Beizen, Modeling Underground Coal Gasification, Ph.D. thesis, Delft University of Technology, Delft, Netherlands, 1996.

[16] S. Daggupati, R. N. Mandapati, S. M. Mahajani, A. Ganesh, D. Mathur, R. Sharma, P. Aghalayam, Laboratory studies on combustion cavity growth in lignite coal blocks in the context of underground coal gasification, Energy 35 (2010) 2374 – 2386.

[17] V. Prabu, S. Jayanti, Laboratory scale studies on simulated underground coal gasification of high ash coals for carbon-neutral power generation, Energy 46 (2012) 351 – 358.

[18] K. Kostúr, J. Kačúr, The monitoring and control of underground coal gasification in laboratory conditions, Acta Montanistica Slovaca 13 (2008) 111–117.

[19] K. Kostur, J. Kacur, Development of control and monitoring system of UCG by promotic, in: 2011 12th International Carpathian Control Conference (ICCC), 2011, pp. 215 –219.

[20] K. J. Aström, T. Hägglund, PID Controllers: Theory, Design, and Tuning, 2 ed., Instrument Society of America, Research Triangle Park, NC, 1995.

[21] I. U. Vadim, Survey paper variable structure systems with sliding modes, IEEE Transactions on Automatic control 22 (1977).

[22] V. I. Utkin, Sliding modes in control and optimization, volume 116, Springer-Verlag Berlin, 1992.

[23] A. Arshad, A. Bhatti, R. Samar, Q. Ahmed, E. Aamir, Model development of ucg and calorific value maintenance via sliding mode control, in: 2012 International Conference on Emerging Technologies (ICET), 2012, pp. 1–6.

[24] W. Perruquetti, Sliding Mode Control in Engineering, Marcel Dekker, Inc., New York, NY, USA, 2002.

[25] V. I. Utkin, J. Guldner, J. Shi, Sliding Mode Control in Electromechanical Systems, Taylor and Francis, London, 1999.

[26] G. Bartolini, A. Ferrara, E. Usai, Second order vsc for non linear systems subjected to a wide class of uncertainty conditions, in: 1996 IEEE International Workshop on Variable Structure Systems, 1996, pp. 49–54.

[27] A. A. Uppal, A. I. Bhatti, E. Aamir, R. Samar, S. A. Khan, Control oriented modeling and optimization of one dimensional packed bed model of underground coal gasification, Journal of Process Control 24 (2014) 269–277.

[28] ASTM, D388-12, Standard Classification of Coals by Rank. ASTM International, West Conshohocken, PA (2012).

[29] A. Levant, Sliding order and sliding accuracy in sliding mode control, International Journal of Control 58 (1993) 1247–1263.

[30] L. Fridman, A. Levant, Higher order sliding modes, in: Sliding Mode Control in Engineering, Marcel Dekker, Inc., New York, NY, USA, 2002, pp. 53–101.

[31] C. Thorsness, E. Grens, A. Sherwood, A One Dimensional Model for In-Situ Coal Gasification, Technical Report UCRL-52523, Lawrence Livermore National Laboratory, Livermore, CA, 1978.

[32] M. Hosea, L. Shampine, Analysis and implementation of TR-BDF2, Applied Numerical Mathematics 20 (1996) 21 – 37.

[33] D. U. Olness, L. L. N. Laboratory, The Podmoskovnaya underground coal gasification station, Livermore, Calif. : Lawrence Livermore Laboratory, University of California, 1981.

[34] M. Blinderman, D. Saulov, A. Klimenko, Forward and reverse combustion linking in underground coal gasification, Energy 33 (2008) 446 – 454.

[35] G. E. I. T. EUROPE, GAS 3100 R Coal gas/Syngas 19-3U Analyser, Gas Engineering and Instrumentation Technologies Europe, B-3380 Bunsbeek, Belgium, 2011.

[36] P. T. Boggs, J. W. Tolle, Sequential quadratic programming, Acta Numerica 4 (1995) 1–51.

[37] L. van Reeuwijk, Guidelines for quality management in soil and plant laboratories, Food & Agriculture Org., 1998.

[38] V. Utkin, On convergence time and disturbance rejection of super-twisting control, IEEE Transactions on Automatic Control 58 (2013) 2013–2017.

[39] S. Boyd, L. Vandenberghe, Convex Optimization, Cambridge University Press, 2004.

[40] K. Morris, Control of systems governed by partial differential equations, in: Electrical Engineering Handbook, CRC Press, 2010, pp. 1–37.

View publication stats